Am J Physiol Lung Cell Mol Physiol 313: L581–L591, 2017.
First published June 22, 2017; doi:10.1152/ajplung.00074.2017.

RESEARCH ARTICLE | *Age-Related Dysfunction in Lung Barrier Function in Health and Disease*

Cigarette smoke disrupts monolayer integrity by altering epithelial cell-cell adhesion and cortical tension

Kristine Nishida,[1]* Kieran A. Brune,[1]* Nirupama Putcha,[1] Pooja Mandke,[1] Wanda K. O'Neal,[2] Danny Shade,[1] Vasudha Srivastava,[3] Menghan Wang,[1] Hong Lam,[4] Steven S. An,[4] M. Bradley Drummond,[2] Nadia N. Hansel,[1] Douglas N. Robinson,[1,3] and Venkataramana K. Sidhaye[1,4]

[1]*Department of Medicine, School of Medicine, Johns Hopkins University, Baltimore, Maryland;* [2]*Marsico Lung Institute, Department of Medicine, University of North Carolina, Chapel Hill, North Carolina;* [3]*Department of Cell Biology, School of Medicine, Johns Hopkins University, Baltimore, Maryland; and* [4]*Department of Environmental Health and Engineering, School of Public Health, Johns Hopkins University, Baltimore, Maryland*

Submitted 23 February 2017; accepted in final form 10 June 2017

Nishida K, Brune KA, Putcha N, Mandke P, O'Neal WK, Shade D, Srivastava V, Wang M, Lam H, An SS, Drummond MB, Hansel NN, Robinson DN, Sidhaye VK. Cigarette smoke disrupts monolayer integrity by altering epithelial cell-cell adhesion and cortical tension. *Am J Physiol Lung Cell Mol Physiol* 313: L581–L591, 2017. First published June 22, 2017; doi:10.1152/ajplung.00074.2017.—Chronic obstructive pulmonary disease (COPD) is a major cause of morbidity and mortality. Cigarette smoke (CS) drives disease development and progression. The epithelial barrier is damaged by CS with increased monolayer permeability. However, the molecular changes that cause this barrier disruption and the interaction between adhesion proteins and the cytoskeleton are not well defined. We hypothesized that CS alters monolayer integrity by increasing cell contractility and decreasing cell adhesion in epithelia. Normal human airway epithelial cells and primary COPD epithelial cells were exposed to air or CS, and changes measured in protein levels. We measured the cortical tension of individual cells and the stiffness of cells in a monolayer. We confirmed that the changes in acute and subacute in vitro smoke exposure reflect protein changes seen in cell monolayers and tissue sections from COPD patients. Epithelial cells exposed to repetitive CS and those derived from COPD patients have increased monolayer permeability. E-cadherin and β-catenin were reduced in smoke exposed cells as well as in lung tissue sections from patients with COPD. Moreover, repetitive CS caused increased tension in individual cells and cells in a monolayer, which corresponded with increased polymerized actin without changes in myosin IIA and IIB total abundance. Repetitive CS exposure impacts the adhesive intercellular junctions and the tension of epithelial cells by increased actin polymer levels, to further destabilize cell adhesion. Similar changes are seen in epithelial cells from COPD patients indicating that these findings likely contribute to COPD pathology.

cigarette smoke; epithelial barrier; cortical tension; E cadherin; COPD

CHRONIC OBSTRUCTIVE PULMONARY disease (COPD) is the third leading cause of death in the US (26). Cigarette smoke (CS) is the primary agent that drives disease development and progression (2, 10, 29, 32, 44). CS affects the entire respiratory epithelium and promotes both chronic bronchitis through airway wall remodeling and increased mucous secretion (4), as well as emphysema through destruction of alveolar walls (18, 39). A recent study demonstrates that current and former smokers with preserved lung function have more respiratory symptoms, greater number of respiratory exacerbations, and greater airway wall thickening than healthy controls who have never smoked (43). Thus the scope of CS-related lung disease may be larger than originally thought.

The airway epithelium, situated at the interface between the external environment and the lung parenchyma, acts as a barrier that protects the subepithelial tissue from inhaled noxious stimuli. Three intercellular junctional complexes (the tight junctions, adherens junctions, and desmosomes) join neighboring cells together to form this barrier. In response to repetitive smoke exposure, decreases in several epithelial tight junction and adherens junction proteins have been observed (15, 16, 31, 34, 38). However, the effects of the changes on the actin cytoskeleton, which interacts with these junctional proteins to cause CS to compromise monolayer integrity, are poorly understood.

E-cadherin (encoded by *CDH1*) is a key transmembrane protein in the adherens junction complex. It contains an extracellular domain that joins neighboring cells and an intracellular domain that links to the cell's actin cytoskeleton. Normally, this protein is inserted in the membrane where it mediates cell adhesion, but upon proteolytic cleavage, a shorter soluble form is generated that weakens cell-cell adhesion, influences its interaction with the actin cytoskeleton, and leads to the initiation of signaling cascades important in tissue repair (17, 30, 46). E-cadherin is thought to play a role in small airway remodeling with increased epithelial-to-mesenchymal-transition in response to CS and in COPD (24). Moreover, of 114 plasma biomarkers studied in the COPDGene cohort, decreased peripheral blood CDH1 levels correlated with increased signs of emphysema (7). CS decreases E-cadherin (24, 27), but it is not known whether this decrease influences the ability of cells to form a tight monolayer.

* K. Nishida and K. A. Brune contributed equally to this work.

Address for reprint requests and other correspondence: V. K. Sidhaye, Johns Hopkins University, Div. of Pulmonary and Critical Care Medicine, 615 N. Wolfe St., E7626, Baltimore, MD 21205 (e-mail: vsidhay1@jhmi.edu).

E-cadherin's extracellular domains form catch-slip bonds to link neighboring epithelial cells together. These bonds are stabilized by linking E-cadherin's intra-cytoplasmic tail to the cell's actin-myosin cytoskeleton (5, 6, 23, 45). The cell cortex, the thin outermost layer of the cytoskeleton that is tethered to the plasma membrane, is composed of densely packed cross-linked actin filaments, myosin II motors, and actin-binding proteins. This network of proteins creates contractility and tension in the cell which maintains cell shape. Many protein-protein interactions are stabilized by an optimal level of cortical tension (8), and for E-cadherin to provide strong sustained adhesion between epithelial cells, it must be coupled to the actin cytoskeleton (9). In a homeostatic state, the adherens junctions are stabilized by a balance between the adhesive forces pulling cells together and the opposing contractility and tension in the cell. Extreme tension (either too high or too low) weakens the adhesive bonds, either by failing to stabilize them (too low cortical tension) or by overwhelming them so that they break (too high cortical tension) (41). Thus this cortical tension, exerted by cytoskeletal proteins, is essential to cellular shape and adhesive systems. Cigarette smoke reduces the abundance of key adhesive proteins (24, 27, 40), yet how this influences the cell's cortical tension has not been explored. Therefore, we hypothesized that cigarette smoke alters monolayer integrity by increasing cell contractility and tension, thereby decreasing cell adhesion. These combined changes lead to sustained increases in epithelial monolayer permeability in the airways of patients with COPD.

MATERIALS AND METHODS

Airway epithelial cell culture. Primary normal human bronchial epithelial (NHBE) cells (Lonza) or primary epithelial cells isolated from bronchial brushings of normal or COPD patients (former smokers ages 50–68 with a 25- to 40-pack year smoking history and Gold Stage II–III disease) were grown on collagen-coated inserts (Falcon) at 37°C with 5% CO_2 in bronchial epithelial growth media (Lonza). Institutional approval for the use of materials and data from human subjects has been obtained. Once cells formed a confluent monolayer, they were allowed to differentiate on air-liquid interface (ALI). All primary cells (either commercially obtained or patient-derived) were analyzed after 4–6 wk on ALI, at which time the cells are terminally differentiated, form a tight monolayer, with optimal ciliogenesis, ciliary beat frequency and air-surface liquid height as described in the literature (13, 42). Cells were harvested and lysed using RIPA buffer, and protein yield was quantified using the BCA protein assay kit (Thermo Scientific).

Immortalized human airway epithelial cells (HBEC-3KT cells, gift of John Minna, U.T. Southwestern) were cultured on inserts (Falcon) at 37°C with 5% CO_2 in keratinocyte serum-free media with supplements (Invitrogen). These cells are a patient-derived primary airway epithelial cell line immortalized with hTERT and cdk4, yet preserve epithelial properties with tight junction and adherens junction formation (14, 25). Cells were harvested and lysed using RIPA buffer and protein yield was quantified as above.

Lung tissue sections. Fresh frozen tissue sections or paraffin embedded tissue sections from healthy controls and from patients with COPD were obtained from the Lung Tissue Research Consortium (LTRC). The healthy controls had no known history of lung disease. The COPD patients had an FEV_1 between 50 and 80% and had a 30–50 pack year smoking history.

Cigarette smoke exposure. For whole CS experiments, cells were exposed to CS in a smoke chamber (Vitrocell). The Vitrocell smoke chamber delivers either whole CS or humidified air to the apical surface of the cell monolayer, which closely simulates what smokers experience (1, 22, 33). Briefly, cell inserts with confluent monolayers on ALI for 4–6 wk were then placed in the Vitrocell smoke chamber and CS or humidified air was puffed onto the apical surface of the epithelial monolayer. One CS exposure consisted of 2 cigarettes which each burned for ~8 min using the ISO puff regimen (one 35-ml puff every 60 s with an 8-s exhaust). A minimum of 2 h elapsed between consecutive smoke exposures. Control inserts were exposed to humidified air in the chamber and 10 min of humidified air was considered 1 exposure.

For experiments using cigarette smoke extract (CSE), 100% CSE was produced by burning 1 research cigarette (University of Kentucky research cigarettes) through peristaltic pumping into 25 ml of cell-specific media. The peristaltic pump was programmed to burn one cigarette in 6 min; 100% CSE was diluted to a working concentration of 10% using cell specific media. One milliliter of 10% CSE was applied to the apical surface of a 6-well insert containing a confluent monolayer. A 2-h incubation period was considered 1 CSE exposure. Prolonged exposure (CSE ×3) was carried out over 2 days as follows: on *day 1*, cells were incubated in 10% CSE for 2 h followed by a 2-h rest period in fresh media, followed by 2 h in 10% CSE. CSE was removed overnight and cells were incubated in fresh media over this time period. On *day 2*, the cells were exposed to 4 h of 10% CSE. For control inserts, 1 ml of cell-specific media was applied to the apical surface, for matching time points to the CSE-exposed cells.

FITC-dextran paracellular permeability assay. Paracellular permeability was assessed using the FITC-dextran assay, as described previously (35). Briefly, following experimental treatment, basolateral media was removed from the wells and 2 ml of fresh media was added to each well. One milliliter of 4-kDa FITC-Dextran (Sigma) at a final concentration of 0.5 mg/ml was added to the apical surface of the cells and allowed to incubate at 37°C for 30 min, with PBS placed in the basolateral chamber. In addition, 1 ml of 4-kDa FITC-dextran was added to a cell-free insert. Following incubation, 200 μl of basolateral contents was removed from the wells, and fluorescence (ex. 490 nm and em. 530 nm) was measured in triplicate using a fluorimeter. The

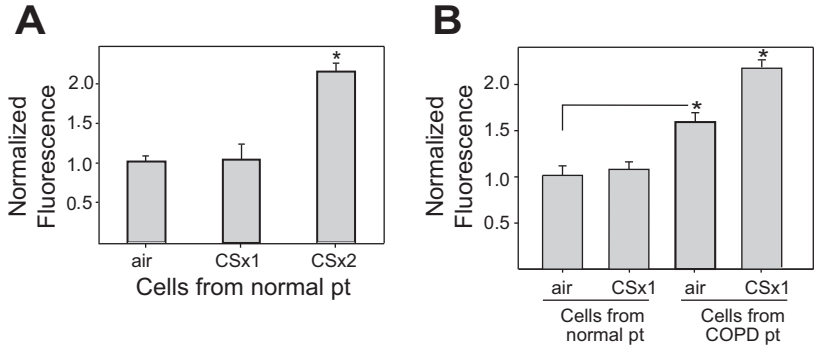

Fig. 1. Cigarette smoke (CS) increases epithelial monolayer permeability. *A*: in normal human airway epithelial cells, one CS exposure did not increase epithelial monolayer permeability as measured by FITC-dextran assay, but 2 CS exposures (2 cigarettes, 2 h rest followed by 2 additional cigarettes) did cause a statistically significant increase in epithelial monolayer permeability (*$P = 0.008$, $n = 4$ patients, with 3 technical replicates per patient). *B*: epithelial cells derived from COPD patients have a more permeable monolayer compared with normal human airway epithelial cells (*$P = 0.02$) and have a further increase in monolayer permeability following one in vitro exposure to CS (*$P = 0.008$) ($n = 4$ patients, with 3 technical replicates per patient).

fluorescence readings were compared with those obtained from PBS alone.

Western analysis. Equal quantities of protein were separated on an acrylamide gel and transferred to a membrane at 47 V overnight at 4°C. Following the transfer, the blots were blocked with 5% milk blocking buffer for 2 h, then incubated in primary antibody (E-cadherin, β-catenin, myosin IIA and B antibodies from Cell Signaling Technology) at a concentration of 1:1,000 for 3 h at room temperature. Blots were washed with 1X phosphate-buffered saline plus 0.2% Tween-20 (PBST), then incubated in appropriate secondary antibody (Bio-Rad) at a dilution of 1:10,000 for 1 h. Blots were washed 3 times with PBST, then visualized on a Li-Cor imager. Images were analyzed using ImageJ software (https://imagej.nih.gov/ij).

Immunofluorescence and immunohistochemistry staining. For immunofluorescence staining, epithelial cell monolayers were fixed in 4% paraformaldehyde in 1X PBS, permeabilized with 0.1% Triton X-100 in 1X PBS, and blocked for 1 h in 1X PBS with 10% goat-serum (blocking solution). The primary antibody, diluted to 1:200 in blocking solution, was incubated on the epithelial cell monolayer for 1 h at room temperature. The cells were then washed with PBS and incubated with secondary antibody for 1 h at room temperature. The cell monolayer was then washed and mounted on a slide. Slides were imaged using a Zeiss 510 confocal microscope and images were analyzed using ImageJ software.

For immunohistochemistry staining, tissue sections were first deparaffinized using xylene and ethanol followed by antigen retrieval with steamed citrate. Tissue sections were blocked for 30 min with Dako dual enzyme block followed by a 24-h incubation period in primary antibody (E-cadherin or β-catenin from Cell Signaling Technology), diluted to appropriate final concentration in PBS containing 0.3% Triton and 1% bovine serum albumin (BSA). Following 3 washes in Triton/BSA PBS, sections were incubated at room temperature for 1 h with a biotinylated goat anti-rabbit secondary antibody (diluted in Triton/BSA PBS). Sections were incubated in avidin-biotin

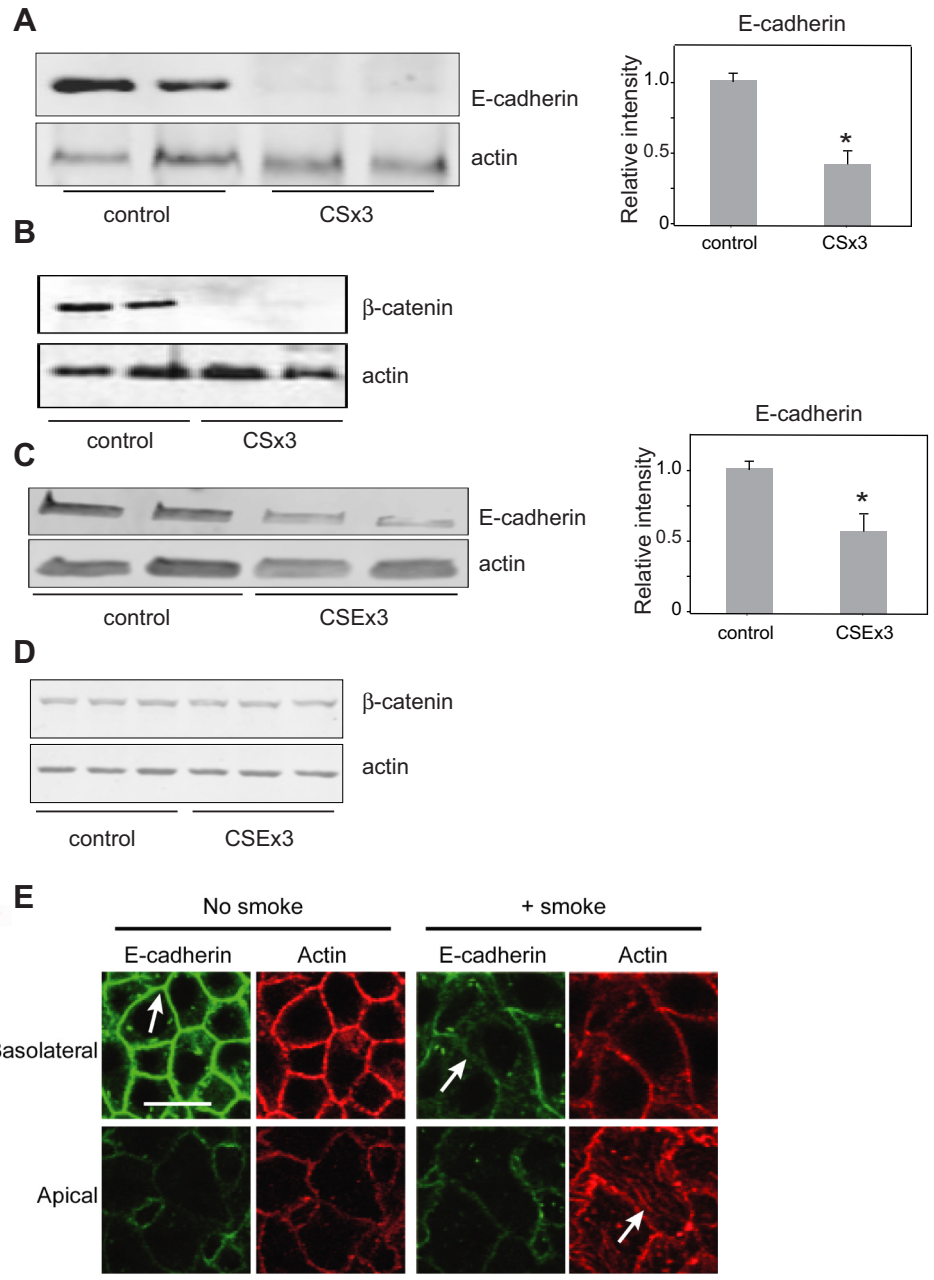

Fig. 2. Cigarette smoke alters adherens junction proteins. *A, left*: representative Western analysis showing a reduction in total E-cadherin protein in NHBE cells following 3 exposures to whole CS in the Vitrocell smoke chamber. *A, right*: densitometry measurement of E-cadherin levels, $*P < 0.05$, $n = 10$. *B*: Western analysis showing a reduction in total β-catenin in NHBE cells following 3 exposures to whole CS in the Vitrocell smoke chamber. $n = 3$ patients. *C, left*: representative Western analysis showing reduction in total E-cadherin in HBEC-3KT cells following 3 exposures to 10% CSE. *C, right*: densitometry measurement of E-cadherin levels, $*P < 0.05$, $n = 10$. *D*: representative Western analysis showing no change in total β-catenin in HBEC-3KT cells after 3 exposures to 10% CSE. $n = 3$. *E*: immunofluorescence of NHBE cells shows that in normal cells E-cadherin is enriched along the basolateral membrane (arrow); representative image is shown, $n = 8$. Following 2 exposures to whole CS, there is a reduction of E-cadherin along this surface (arrow). In addition, there is evidence of actin stress fibers across the apical surface of the epithelium after CS exposure (arrow). Scale bar, 20 μm.

peroxidase complex for 30 min at room temperature, followed by washing in PBS. The DAB chromogen was applied to sections and slides were imaged.

Cortical tension and cell stiffness measurements. Cells were dissociated with trypsin (0.025%) for 5 min, and once dissociated collected with trypsin neutralizing solution before resuspending in media for cortical tension measurements. Cortical tension was measured in individual cells using micropipette aspiration (MPA) (19, 20, 37). Incremental suction pressures were applied to the cell cortex using a micropipette of defined radius (8–9 μm radius, R_p) until the critical pressure (ΔP), where L_p (length of the cell inside the pipette) equals R_p, was reached. The effective cortical tension (T_{eff}) was calculated by applying the Young-Laplace equation: $\Delta P = 2T_{eff}(1/R_p - 1/R_c)$ where ΔP is the critical pressure at which $L_p = R_p$, and R_c is the radius of the cell. Image analysis was performed using ImageJ software.

The stiffness of cells in a monolayer was measured using magnetic twisting cytometry (MTC). RGD-coated ferromagnetic beads were applied to the epithelial monolayer and bound to the cell membrane through integrin receptors. The beads were magnetized in the horizontal plane using a brief large magnetic pulse. Following magnetization, a sinusoidal twisting current was applied perpendicular to the magnetic field, which caused the beads to oscillate creating stress in the epithelial monolayer, and the bead displacement was measured.

Assembled actin measurement. Equal number of cells were lysed on ice for 10 min in lysis buffer containing 50 mM PIPES (pH 6.8) and 0.5% Triton X-100. Following lysis, the samples were centrifuged at 15,000 *g* for 5 min at 4°C. After centrifuging, the supernatant containing unassembled G-actin was transferred to a fresh tube, 1 μl of RNase A was added, and the sample was boiled for 5 min. The pellet containing assembled F-actin was resuspended in lysis buffer without Triton X-100, 1 μl of RNase A was added, and the sample was boiled for 5 min. Equal amounts of sample buffer were added to the samples, and the samples were separated on an acrylamide gel and probed for actin.

E-cadherin knockdown. Cells were transfected with 1×10^6 PFU of either a human *cdh1* shRNA adenovirus for gene knockdown or a scrambled shRNA for control. Both adenoviruses also expressed a green fluorescent protein (GFP) marker so that the infected cells could be identified. After 24 h, the transfection efficiency was measured with direct visualization using fluorescence microscopy as well as Western analysis. Only fluorescently labeled cells were used for MPA.

Serum E-cadherin analysis. Serum was obtained from participants in the Subpopulations and Intermediate Outcome Measures in COPD Study (SPIROMICS), a multicenter cohort study including current and former smokers (>20 pack years) with and without airways obstruction, who completed extensive phenotyping including questionnaire, biomarker analysis, spirometry, CT scan, and outcome assessment. COPD was defined as post bronchodilator FEV_1/FVC ratio less than 0.7 and an FEV_1 less than the lower limits of normal. The study and exclusion criteria have been described previously (11). Serum E-cadherin levels were determined using a multiplex assay created by Myriad-RBM (Austin, TX). Serum E-cadherin levels were available from 1,677 participants with and without COPD at baseline. Chest CT scans were performed as described previously (11) and total percentage of emphysema was calculated using VIDA software (Apollo, VIDA Diagnostics), and defined as percentage of voxels less than 950 Houndsfield units in the inspiratory phase.

Statistical analysis. For analysis of the epithelial cell data, multiple groups were compared using one-way ANOVA with Bonferroni correction for multiple pairwise comparisons when data were normally distributed or with Kruskal-Wallis assessment when data were skewed. Two groups were compared using the Student's *t*-test or the Mann-Whitney rank sum test depending on normal vs. skewed distribution, respectively. Baseline data from SPIROMICS were analyzed using Stata 12 statistical software package (College station, TX, 2011). To analyze associations of E-cadherin level with COPD case status among all participants (controls without smoking history, controls with smoking history, and COPD cases), multivariable logistic regression models adjusting for smoking status, age, and race (African American vs. all others) as well as batch number (for biomarker run) were constructed. Multivariable linear regression models were constructed adjusting for the same covariates in addition to COPD case status, to determine associations between E-cadherin levels with percentage emphysema.

RESULTS

Cigarette smoke increases epithelial monolayer permeability without causing increased cell death. In NHBE cells, one CS exposure in the Vitrocell smoke chamber did not significantly increase epithelial monolayer permeability as measured by the FITC-dextran permeability assay when compared with epithelial cells exposed to humidified air (Fig. 1*A*). Two CS exposures with a 1-h rest period between exposures resulted in increased epithelial monolayer permeability when compared with cells exposed to humidified air without causing increased

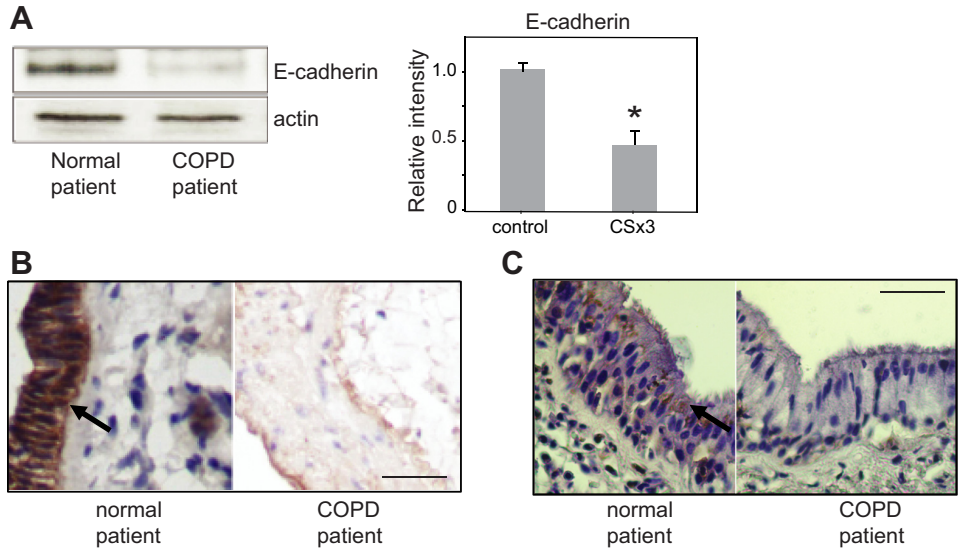

Fig. 3. E-cadherin is reduced in COPD patients. *A, left*: representative Western analysis showing a reduction in total E-cadherin protein in a COPD patient compared with a patient with no history of COPD. Cell pellets were obtained from bronchial brushings. *A, right*: densitometry measurement of E-cadherin levels, $n = 4$ patient replicates. $^*P < 0.05$. *B*: immunohistochemistry of lung tissue sections demonstrating that in normal individuals E-cadherin is enriched along the lateral surface. In tissue sections from patients with COPD, E-cadherin staining is reduced along this surface. *C*: in tissue sections from patients with COPD, β-catenin staining is less prominent in the epithelium of COPD patients compared with lung sections from normal subjects. $n = 8$ patients/condition were analyzed for *B* and *C*. Scale bar, 50 μm.

cell death (Fig. 1*A*). Similar changes in monolayer permeability were seen following three smoke exposures.

In contrast, epithelial cells isolated from COPD patients at baseline formed a more permeable monolayer, and these cells were more susceptible to CS in vitro when compared with normal human airway epithelial cells (Fig. 1*B*). Whereas normal human bronchial epithelial cells required at least two CS exposures to cause statistically significant changes in epithelial monolayer permeability, epithelial cells isolated from COPD patients required only one smoke exposure to cause statistically significant changes in permeability. Thus we demonstrate that epithelial cells isolated from patients with COPD have a sustained change in the epithelium compared with cells from normal hosts despite being cultured in vitro.

Adherens junction proteins are altered following cigarette smoke exposure and in COPD patients. To examine the molecular mechanisms underlying these permeability changes, we examined CS-induced changes in E-cadherin and β-catenin levels. NHBE cells exposed to repetitive CS had a reduction in total E-cadherin (Fig. 2*A*) and the E-cadherin-binding protein, β-catenin (Fig. 2*B*). This reduction in total E-cadherin and β-catenin was seen after two and three CS exposures, which corresponded to the changes in permeability described above. In addition, similar to what was seen following whole CS exposure, HBEC-3KT cells exposed to repetitive CSE in 2-h blocks over 2 days also had a reduction in total E-cadherin (Fig. 2*C*), although total β-catenin was largely unchanged (Fig. 2*D*). Moreover, we found that after two exposures to whole CS, E-cadherin becomes reduced along the basolateral membrane (Fig. 2*E*). After both CS or CSE exposure, we have assessed cell viability using trypan blue, without evidence of significant differences in cell death. Whereas relative changes in the distribution of polymerized actin are visualized, there is no clear evidence of altered levels of total actin. Therefore, following repetitive CS exposure (including whole CS and CSE), epithelial monolayer permeability increases as E-cadherin levels decrease.

In epithelial cells isolated from patients with COPD, total E-cadherin was also decreased in whole cell extracts (Fig. 3*A*). Moreover, immunohistochemistry of lung tissue sections showed that E-cadherin was reduced altogether in tissues from COPD patients, whereas in normal lung epithelia E-cadherin is enriched (arrow) along the tissue border (Fig. 3*B*). In addition, β-catenin staining was also reduced along the epithelial border in tissue sections from COPD patients when compared with normal control patients with no history of COPD (Fig. 3*C*). These findings demonstrate that the reduction in these proteins is not simply due to an overall decrease in the number of epithelial cells in patients with COPD, but due to decreased protein levels in the epithelial cells themselves.

Cigarette smoke alters the cortical tension and stiffness of airway epithelial cells. As adhesion between cells is dictated both by intercellular proteins as well as the tension of the cell to allow for contact between cell surfaces, we measured the cortical tension and cell stiffness, a related parameter, to discern the impact of CS on these mechanical parameters. The tension and stiffness of cells in a monolayer can be measured using magnetic twisting cytometry (MTC) in which magnetized beads are applied to the epithelial monolayer and made to oscillate by applying a twisting force. This assay cannot be performed in cells living at the air-liquid interface as the laxity of the transwell membrane is greater than the displacement of the beads under torque. Therefore, we used HBEC-3KT cells grown in 6-well culture dishes for this assay. MTC was performed on cell monolayers under control, short- or long-term CSE exposure conditions. Following a short-term exposure to CSE, cell stiffness was reduced in the epithelial mono-

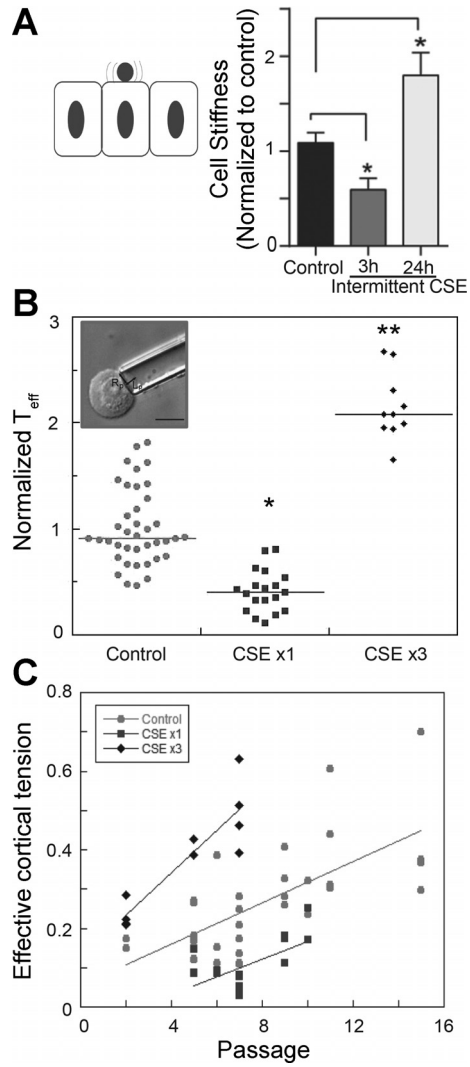

Fig. 4. Repetitive CS exposure increases the tension of individual cells and cells in a monolayer. *A*: stiffness of HBEC-3KT cells in a monolayer is determined using MTC in which ferromagnetic beads are applied to the monolayer surface and displacement of beads is measured after a sinusoidal twisting force is applied to the beads. Following short-term exposure to CSE, cells in an epithelial monolayer have a statistically significant decrease in stiffness compared with cells in untreated monolayers. In contrast, following prolonged CSE exposure, cells within the epithelial monolayer show a statistically significant increase in stiffness compared with untreated controls (*$P <$ 0.005). *B*: MPA was used to measure the cortical tension of individual cells. Using a micropipette of a set radius (*inset*), force is applied to the surface of the cell causing a portion of the cell membrane to pull into the pipette. Scale bar, 10 μm. Following short-term exposure to CSE, cortical tension decreases ~2-fold in smoke-exposed cells compared with unexposed cells (*$P <$ 0.005). In contrast, following prolonged exposure to CSE, cortical tension increases ~2-fold in smoke exposed cells compared with unexposed cells (**$P <$ 0.005). *C*: the cortical tension of cells increases in a near linear fashion with cell passage. Cortical tension measurements were normalized to the calculated value at each passage number based upon the linear fit to the entire data set.

layer when compared with cells exposed to media alone. In contrast, following exposure to intermittent CSE over a 24-h period, cell stiffness increased when compared with cells exposed to media alone (Fig. 4*A*).

To determine if these changes in cell stiffness were dependent on cell-cell adhesion or were a cell autonomous effect, we measured the cortical tension of HBEC-3KT cells exposed to short- and long-term CSE using micropipette aspiration (MPA) (Fig. 4*B*). This assay is performed on live cells that have been detached from the transwell membrane. In normal human epithelial cells, we found a ~2-fold decrease in the normalized cortical tension of cells exposed to short-term CSE exposure when compared with cells exposed to media alone (Fig. 4*B*). It is worth noting that the cortical tension measurements were performed on cells over a wide passage range (2–15). We observed that passage number had a profound impact on the cortical tension of the cells, increasing with passage number (Fig. 4*C*). In fact, when we plotted the tension measurements as a function of passage number, we found a strong linear trend. Therefore, to address this and to avoid having to select data, we normalized the values against the calculated value at each passage number based upon the linear fit. Nevertheless, the measured decrease in normalized cortical tension indicates that cells exposed to a short CSE exposure were much softer and more deformable than unexposed cells. When the cells were exposed to long-term CSE exposure, we detected a 2-fold increase in normalized cortical tension as compared with matched control cells (Fig. 4*B*). This increase in cortical tension indicates that cells exposed to prolonged CSE were much stiffer and less deformable. Multiple measurement techniques indicate that individual cells and cells in a monolayer display a biphasic biomechanical response to CSE.

Epithelial cytoskeletal remodeling occurs in response to repetitive cigarette smoke and in COPD. Increases in cortical tension of the cells indicate changes in the actin-myosin cytoskeleton. To understand mechanisms leading to these cytoskeletal changes, we examined the impact of CS on the amount and localization of the myosin II paralogs present in the cells. In HBEC-3KT cells, myosin IIA and IIB levels did not change in response to short- and long-term CSE (Fig. 5, *A* and *B*). To determine if there are changes in myosin II localization, we used terminally differentiated monolayers of NHBE cells, and found myosin IIB is localized along the lateral cell surface (Fig. 6*A*). Following two smoke exposures, myosin IIB was still found along the basolateral surface, without change in distribution of myosin IIB in these cells following smoke exposure. As we did not see changes in myosin II, we then set to determine if there were changes in the polymerization of actin in response to CSE. Following short-term CSE exposure, there was a nonstatistically significant trend toward decreased actin polymerization compared with control cells. Following repetitive CSE, the fraction of assembled actin increased ~50% (Fig. 6, *B* and *C*) indicating that there is dynamic cytoskeletal remodeling with CS which is a mechanism to explain the increase in cortical tension. Furthermore, following repetitive CS exposure there are apical actin stress fibers (Fig. 6*A*).

To determine if these changes seen after subacute cellular exposure represent changes that occur with disease, we studied lung tissue sections from patients with COPD. Myosin IIB and myosin IIC were reduced compared with lung tissue sections from normal patients with no underlying lung disease. Despite this apparent overall reduction in myosin IIB, myosin IIB was preserved in the subapical compartment of the epithelium. In contrast, myosin IIA abundance and distribution appeared unchanged between normal and COPD tissue (Fig. 6*D*). The increased phalloidin staining in COPD tissues compared with normal tissue sections indicates a greater concentration of actin polymerization in the COPD epithelium, indicating that our subacute findings in cells do represent changes seen in patients with COPD (Fig. 6*D*).

E-cadherin and cigarette smoke have independent effects on cortical tension. Although it is known that an optimal cortical tension is required to maintain the intercellular adhesive strength of E-cadherin, the effects of E-cadherin on cortical tension are not known. To determine if the change in cortical tension following CS exposure was due to decreased E-cadherin, cells were transfected with an adeno sh-E-cadherin or an adeno sh-control virus. NHBE cells grown and differentiated on permeable inserts were infected with adeno sh-control or sh-E-cadherin for 24 h and monolayer permeability was measured at 72 h post virus via FITC-dextran assay. Viral transduction resulted in over 50% knockdown of E-cadherin (Fig. 7*A*). Interestingly, there was no difference in FITC dextran permeability between sh-control and sh-E-cadherin treated inserts indicating E-cadherin loss is not sufficient to decrease permeability suggesting more must occur for the increase in

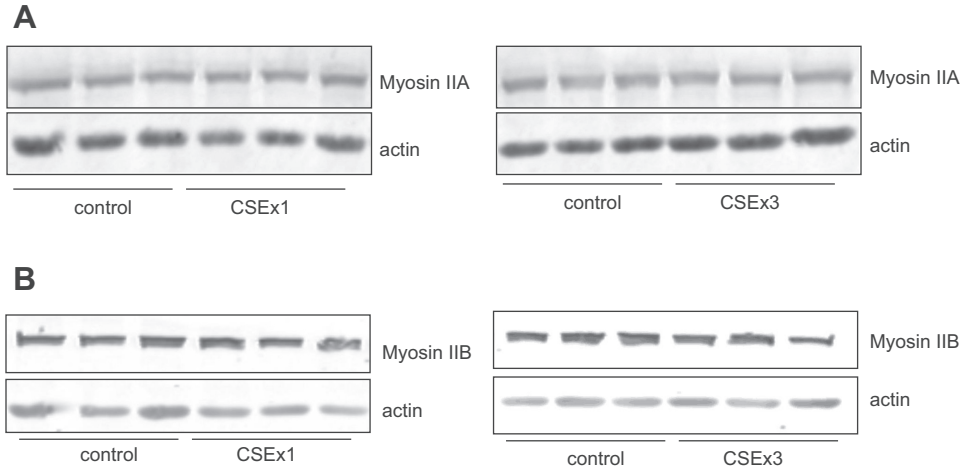

Fig. 5. Cigarette smoke extract does not alter total amount of myosin II. *A, left*: Western analysis showing no change in total myosin IIA following one exposure to CSE ($n = 3$). *A, right*: Western analysis showing no change in total myosin IIA following 3 exposures to CSE ($n = 3$). *B, left*: Western analysis showing no change in total myosin IIB following one exposure to CSE ($n = 3$). *B, right*: Western analysis showing no change in total myosin IIB following 3 exposures to CSE ($n = 3$).

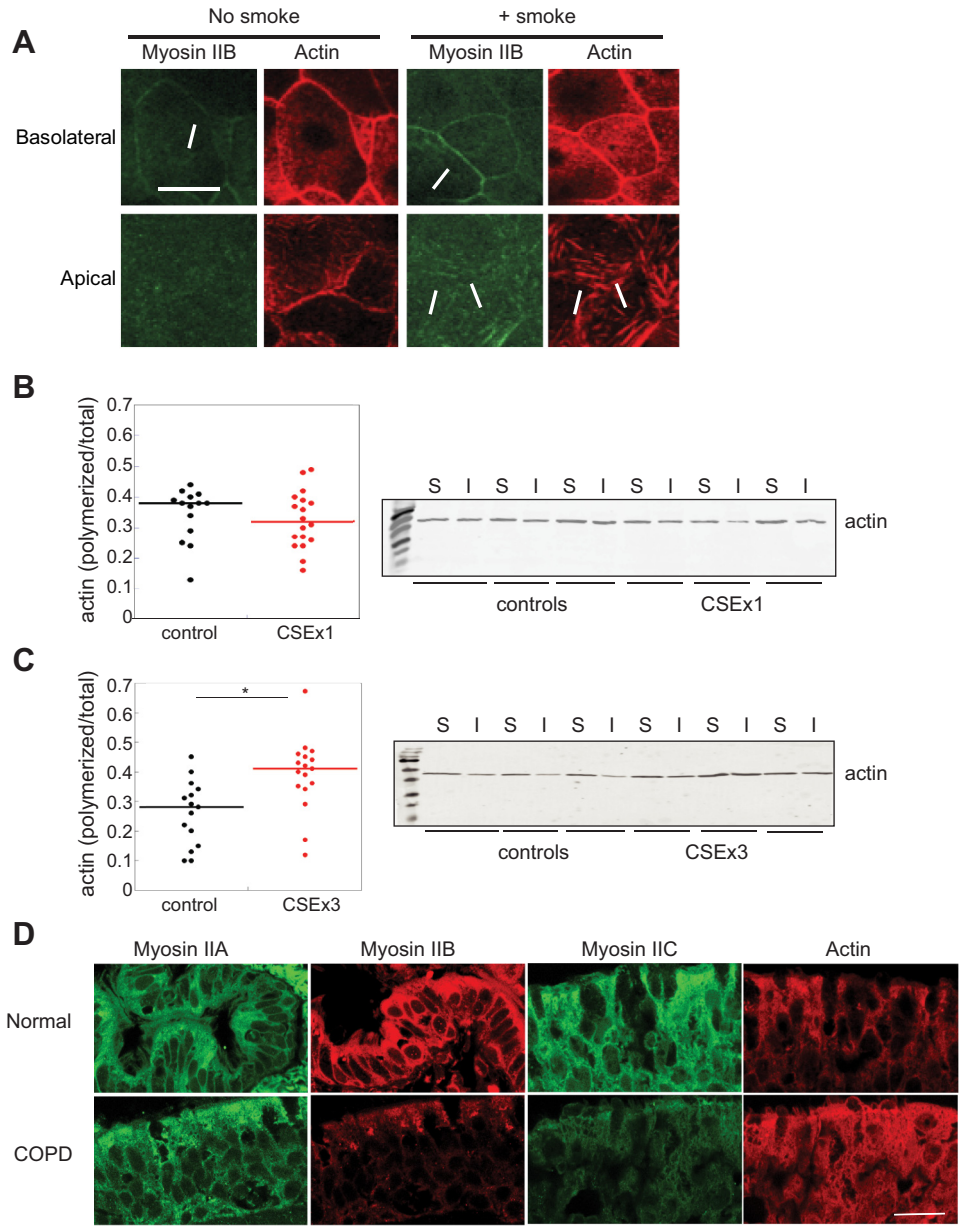

Fig. 6. Cigarette smoke causes cytoskeletal rearrangement. *A*: immunofluorescence of NHBE cells shows that myosin IIB is enriched along the basolateral membrane and apical stress fibers in control cells and following 2 CS exposures (arrows). *B*: following short-term exposure to CSE, the actin polymer fraction was reduced slightly, but this change was not statistically significant ($P = 0.13$, $n = 14$ controls, 18 CSE, representative Western to the right showing soluble and insoluble fractions of actin from a given sample. Total actin is calculated as the summation of soluble and insoluble fraction). *C*: in contrast, following exposure to prolonged CSE, the actin polymer fraction increased ~50% increase (*$P = 0.01$, $n = 15$ controls, 17 CSE; representative Western to the right showing soluble and insoluble fractions of actin from a given sample. Total actin is calculated as the summation of soluble and insoluble fraction). *D*: immunofluorescence imaging of lung sections from patients with COPD showing an overall reduction in myosin IIB and myosin IIC compared with tissue sections from patients without COPD. Despite the overall decrease, myosin IIB appears to be relatively well preserved in the apical subcompartment. In contrast, myosin IIA does not change in its amount or distribution (representative images depicted, $n = 8$ patients/condition). Scale bar, 20 μm.

permeability observed after repetitive smoke (Fig. 7*B*). Knockdown of E-cadherin in cultured cells resulted in a 2-fold reduction in cortical tension in individual cells when compared with control cells (Fig. 7). Since these cells were from limited passage numbers (7–10), these cells were normalized to the average control for each passage number. Following exposure to long-term CSE, the adeno sh-control cells exposed to CSE had a twofold increase in cortical tension when compared with unexposed adeno sh-control cells similar to our findings in cells not transfected with adenovirus. Moreover, both adeno sh-control and adeno sh-E-cadherin cells had a twofold increase in cortical tension from their baseline levels following long-term CSE exposure. This similar twofold increase in cortical tension, albeit from different baselines, indicates that CSE and E-cadherin have independent effects on the cortical tension of the cell.

E-cadherin levels are altered in the serum of individuals with COPD. To determine if the observed changes in E-cadherin were recapitulated in a larger group of patients, we analyzed 1,677 individuals in the SPIROMICS cohort with available serum E-cadherin levels (reported as ng/ml). The demographics of this cohort are described in Table 1. Briefly, the cohort consisted of 1,677 individuals, 1,049 of whom had COPD. The mean age of the cohort was 64 yr, 46% were female and 17.6% were African American. Mean serum E-cadherin level in the full cohort was 3,740.8 ng/ml (SD 1,577.9) and 3,706.8 ng/ml (SD 1,599.2) among those with COPD. After adjustment for smoking status, age and race (African American vs. all others) as well as batch number (for biomarker run), individuals with COPD had lower levels of E-cadherin compared with controls (β, model coefficient representing the difference is −225.06 ng/ml; 95% confidence

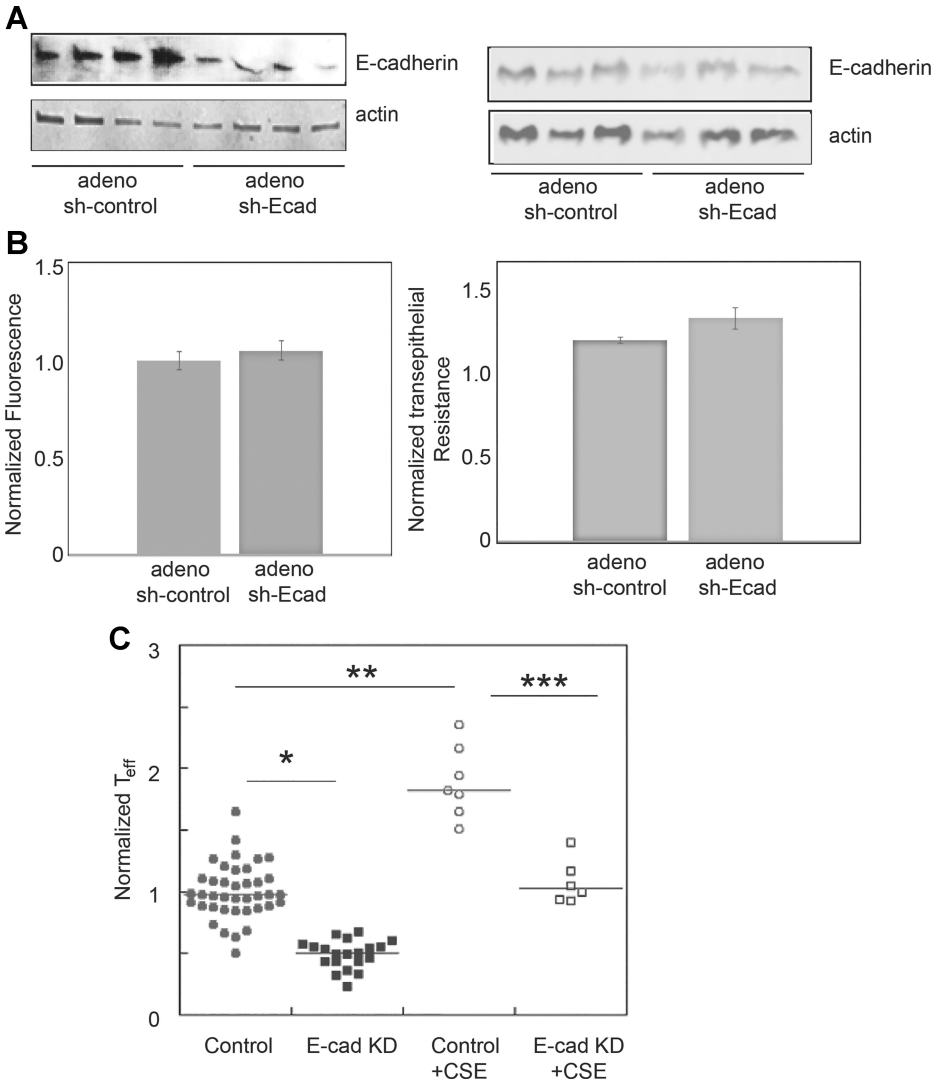

Fig. 7. E-cadherin and cigarette smoke have opposing effects on the cell's cortical tension. *A*: knockdown of E-cadherin in HBE3KT cells (*left*) and NHBE cells (*right*) using adenoviral transduction of either a scrambled shRNA control virus or shRNA directed against E-cadherin (CHD1) causes over 50% knockdown of E-cadherin protein at 72 h postincubation. *B*: knockdown of E-cadherin does not increase paracellular permeability of decrease transepithelial resistance. *C*: E-cadherin knockdown (KD) results in a twofold reduction in cortical tension of cells ($*P < 0.005$). Prolonged CSE exposure (2 exposures) results in a twofold increase in cortical tension for both control ($**P < 0.005$) and E-cadherin knockdown, relative to the untreated comparators for each cell type (each data point shows measurement of an individual cell, averaged over 2 or 3 measurements. Data show aggregated measurements over 3–5 different experiments). $***P < 0.005$.

interval −402.01, −48.11; $P = 0.013$). Additionally, higher E-cadherin levels were associated with a trend toward a lower percentage of emphysema. Specifically, after adjustment for the above covariates as well as COPD case status, a 100 ng/ml increase in E-cadherin level in the serum was associated with a lower percentage of emphysema on CT (β −0.028%, 95% confidence interval −0.056 to 0.00095, $P = 0.058$).

DISCUSSION

In this study, we describe the changes in critical adhesive junction proteins and even more critical changes in the biomechanical properties of airway epithelial cells in response to repetitive CS exposure to disrupt monolayer integrity. Although the in vitro exposures occur on a subacute time frame, the findings mirror the changes in monolayer integrity measured from cells derived from COPD patients, and alterations in the actin cytoskeleton in immunofluorescence in patient derived tissue, and correlate with serum markers suggesting our model does have relevance to findings in patients with COPD, and likely contribute to COPD pathology.

Acute changes in epithelial permeability in response to CS have been noted (24, 27, 40), with a limited understanding of the mechanisms mediating this change. COPD often develops years after the initial insult, suggesting that repetitive exposure is needed to alter the structure and function of the epithelium. In this study, we found that as few as two CS exposures cause significant increases in monolayer permeability, with alterations in the structure of key adhesive junctions. These changes are also observed in the epithelium of COPD patients without ongoing exposure to tobacco, indicating that they are not just a consequence of acute tobacco exposure. Moreover, to our knowledge, this is the first demonstration that epithelial cells isolated from the airways of patients with COPD have fundamental modifications in monolayer integrity even when isolated and cultured from the patient and appear more susceptible to the harmful effects of CS than normal epithelial cells.

These changes in permeability correspond with reduction in key adhesive junction proteins, namely E-cadherin and β-catenin. These changes are not only seen in epithelial cells exposed to CS, but also in lung sections from COPD patients. Moreover, the reduction in E-cadherin in COPD patients was recapitulated in the SPIROMICS cohort where we observed that COPD patients had lower levels of E-cadherin compared with controls without COPD. These observations show similar

Table 1. *Demographics of individuals in the SPIROMICS study populations*

	COPD	Former and Current Smokers without COPD	*P* Value for Difference
Number	1,049	628	
Age	66.1 (7.80)	60.2 (10.1)	<0.001
Female, *n* (%)	435 (41%)	338 (54%)	<0.001
African American, *n* (%)	134 (13%)	161 (26%)	<0.001
>High school education, *n* (%)	663 (63%)	413 (66%)	0.220
Smoking status, *n* (%)			<0.001
Nonsmoker, *n* (%)	0 (0%)	142 (23%)	
Former smoker, *n* (%)	711 (68%)	257 (41%)	
Current smoker, *n* (%)	338 (32%)	229 (36%)	
Gold category, *n* (%)			<0.001
0	0 (0%)	628 (100%)	
1	257 (24%)	0 (0%)	
2	460 (44%)	0 (0%)	
3	241 (23%)	0 (0%)	
4	91 (9%)	0 (0%)	
BMI	27.5 (5.2)	28.9 (5.2)	<0.001
% Emphysema*	11.0 (11.0)	1.66 (1.90)	<0.001

All values are means (SD) unless otherwise indicated. *%Emphysema defined as percentage of voxels <950 Houndsfield units in the inspiratory phase.

trends to observations from the COPDGene cohort (7), providing essential confirmation that CDH1 levels are observed to be altered in two patient cohorts. Thus alterations on E-cadherin appear to play a role in the pathogenesis of COPD. Although it is not clear how serum E-cadherin levels correlate with cellular levels, a preliminary assessment of 10 patients with matched bronchial brushings and serum showed a linear correlation between the two (data not shown). Although preliminary, with a very small sample size, these findings are provocative and the subject of future investigation.

The binding energies of adhesion proteins, including E-cadherin, are likely too small to account for substantial cell-cell adhesion to cause significant increases in permeability following repetitive CS exposure (12, 21, 36). This is highlighted by our findings that E-cadherin knockdown did not affect FITC dextran permeability. Loss of the adherens junction protein E-cadherin is not significant enough to alter permeability suggesting that tight junctions which comprise the physical barrier between cells in epithelium are fairly stable once they are formed. In this study, we demonstrate that in addition to the intercellular adhesion junctions, CS impacts the cortical tension of airway epithelial cells which stabilizes these intercellular bonds. Although we have identified that a single CS exposure significantly decreases the cortical tension of the cells, this exposure is not associated with increased monolayer permeability, and given that it is a response to a single exposure, likely does not represent a mechanism relevant to COPD pathology. Consistent with this, sh-E-cadherin treated cells that decreased cortical tension did not show changes in monolayer permeability and our studies of other types of epithelia also indicate that reduced cortical tension actually facilitates adhesion formation (3).

In contrast, the increased cellular tension following repetitive CS exposure likely does contribute to the observed increased monolayer permeability. This increased tension drives the cell to take on a more spherical form, reducing the available surface area for cell-cell adhesion. We find that this increased cortical tension corresponds to increased actin polymer levels and stress fiber formation as has been suggested in earlier studies (28). Because we also observed these alterations in airway epithelial tissues from COPD patients, they likely contribute to the pathological tissue remodeling associated with COPD progression. Furthermore, this concept that increased cortical tension opposes adhesion between epithelial cells appears to be generalizable, as similar behaviors have been observed in primary hepatocytes and in the liver (3).

E-cadherin and CS have independent and opposite effects on the biomechanical properties of airway epithelial cells. The loss of E-cadherin following long-term CS exposure and in the airway epithelium of COPD patients might serve as a compensatory mechanical response to the increased contractility and stiffness. The loss of membrane-bound E-cadherin may also free up the protein so that it can be cleaved and solubilized for its participation in tissue repair. Nevertheless, the combination of increased contractility and loss of adhesive proteins may ultimately compromise the changes in tissue integrity observed in COPD.

One important limitation to this study is that the primary cells and tissue sections obtained from COPD patients came from a limited number of donors without a full assessment of the various COPD subtypes, which is beyond the scope of this study. Future studies with samples derived from a larger patient population are required to determine if these changes will persist across different phenotypes of COPD and across patients with different smoking exposures. Despite this limitation, we have developed an in vitro CS exposure model that mimics the epithelial barrier changes seen in patients with COPD. Furthermore, we have shown that CS impacts both the adhesive intercellular junctions and the tension and contractility of epithelial cells. These architectural and mechanical alterations then further destabilize cell-cell adhesion, potentially contributing to COPD pathology.

ACKNOWLEDGMENTS

We thank the SPIROMICS participants and participating physicians, investigators and staff for making this research possible. More information about the study and how to access SPIROMICS data is at www.spiromics.org. We acknowledge the following current and former investigators of the SPIROMICS sites and reading centers: Neil E. Alexis, PhD; Wayne H Anderson, PhD; R. Graham Barr, MD, DrPH; Eugene R. Bleecker, MD; Richard C. Boucher, MD; Russell P. Bowler, MD, PhD; Elizabeth E. Carretta, MPH; Stephanie A. Christenson, MD; Alejandro P. Comellas, MD; Christopher B. Cooper, MD, PhD; David J. Couper, PhD; Gerard J. Criner, MD; Ronald G. Crystal, MD;

Jeffrey L. Curtis, MD; Claire M. Doerschuk, MD; Mark T. Dransfield, MD; Christine M. Freeman, PhD; MeiLan K. Han, MD, MS; Nadia N. Hansel, MD, MPH; Annette T. Hastie, PhD; Eric A. Hoffman, PhD; Robert J. Kaner, MD; Richard E. Kanner, MD; Eric C. Kleerup, MD; Jerry A. Krishnan, MD, PhD; Lisa M. LaVange, PhD; Stephen C. Lazarus, MD; Fernando J. Martinez, MD, MS; Deborah A. Meyers, PhD; John D. Newell Jr, MD; Elizabeth C. Oelsner, MD, MPH; Wanda K. O'Neal, PhD; Robert Paine III, MD; Nirupama Putcha, MD, MHS; Stephen I. Rennard, MD; Donald P. Tashkin, MD; Mary Beth Scholand, MD; J. Michael Wells, MD; Robert A. Wise, MD; and Prescott G. Woodruff, MD, MPH. The project officers from the Lung Division of the National Heart, Lung, and Blood Institute were Lisa Postow, PhD, and Thomas Croxton, PhD, MD. SPIROMICS was supported by contracts from the NIH/NHLBI (HHSN268200900013C, HHSN268200900014C, HHSN268200900015C, HHSN268200900016C, HHSN268200900017C, HHSN268200900018C, HHSN268200900019C, HHSN268200900020C), which were supplemented by contributions made through the Foundation for the NIH from AstraZeneca; Bellerophon Therapeutics; Boehringer-Ingelheim Pharmaceuticals, Inc.; Chiesi Farmaceutici SpA; Forest Research Institute, Inc.; GSK; Grifols Therapeutics, Inc.; Ikaria, Inc.; Nycomed GmbH; Takeda Pharmaceutical Company; Novartis Pharmaceuticals Corporation; Regeneron Pharmaceuticals, Inc.; and Sanofi.

GRANTS

This work was supported by the National Institutes of Health Grants GM-66817 (to D. N. Robinson), HL-107361 (to S. S. An), and HL-124099 (to V. K. Sidhaye)) and FAMRI Grant 90046616 (to V. K. Sidhaye).

DISCLOSURES

No conflicts of interest, financial or otherwise are declared by the authors.

AUTHOR CONTRIBUTIONS

K.N., K.A.B., P.M., D.S., V.S., M.W., and H.L. performed experiments; K.N., K.A.B., N.P., and V.K.S. analyzed data; K.N., K.A.B., N.P., and V.K.S. prepared figures; K.N., N.P., P.M., W.K.O., D.S., V.S., H.L., S.S.A., M.B.D., N.N.H., D.N.R., and V.K.S. edited and revised manuscript; K.N., K.A.B., N.P., P.M., W.K.O., D.S., V.S., H.L., S.S.A., M.B.D., N.N.H., D.N.R., and V.K.S. approved final version of manuscript; K.A.B., S.S.A., N.N.H., D.N.R., and V.K.S. conceived and designed research; K.A.B., N.P., and V.K.S. interpreted results of experiments; K.A.B. and V.K.S. drafted manuscript.

REFERENCES

1. **Adamson J, Thorne D, Errington G, Fields W, Li X, Payne R, Krebs T, Dalrymple A, Fowler K, Dillon D, Xie F, Meredith C.** An inter-machine comparison of tobacco smoke particle deposition in vitro from six independent smoke exposure systems. *Toxicol In Vitro* 28: 1320–1328, 2014. doi:10.1016/j.tiv.2014.06.012.
2. **Arunachalam G, Sundar IK, Hwang JW, Yao H, Rahman I.** Emphysema is associated with increased inflammation in lungs of atherosclerosis-prone mice by cigarette smoke: implications in comorbidities of COPD. *J Inflamm (Lond)* 7: 34, 2010. doi:10.1186/1476-9255-7-34.
3. **Bai H, Zhu Q, Surcel A, Luo T, Ren Y, Guan B, Liu Y, Wu N, Joseph NE, Wang TL, Zhang N, Pan D, Alpini G, Robinson DN, Anders RA.** Yes-associated protein impacts adherens junction assembly through regulating actin cytoskeleton organization. *Am J Physiol Gastrointest Liver Physiol* 311: G396–G411, 2016. doi:10.1152/ajpgi.00027.2016.
4. **Barnes PJ.** Chronic obstructive pulmonary disease. *N Engl J Med* 343: 269–280, 2000. doi:10.1056/NEJM200007273430407.
5. **Bell GI.** Models for the specific adhesion of cells to cells. *Science* 200: 618–627, 1978. doi:10.1126/science.347575.
6. **Borghi N, Sorokina M, Shcherbakova OG, Weis WI, Pruitt BL, Nelson WJ, Dunn AR.** E-cadherin is under constitutive actomyosin-generated tension that is increased at cell-cell contacts upon externally applied stretch. *Proc Natl Acad Sci USA* 109: 12568–12573, 2012. [*Proc Natl Acad Sci USA* 109:19034, 2012.] 10.1073/pnas.1204390109.
7. **Carolan BJ, Hughes G, Morrow J, Hersh CP, O'Neal WK, Rennard S, Pillai SG, Belloni P, Cockayne DA, Comellas AP, Han M, Zemans RL, Kechris K, Bowler RP.** The association of plasma biomarkers with computed tomography-assessed emphysema phenotypes. *Respir Res* 15: 127, 2014. doi:10.1186/s12931-014-0127-9.
8. **Cavey M, Lecuit T.** Molecular bases of cell-cell junctions stability and dynamics. *Cold Spring Harb Perspect Biol* 1: a002998, 2009. doi:10.1101/cshperspect.a002998.
9. **Chu YS, Thomas WA, Eder O, Pincet F, Perez E, Thiery JP, Dufour S.** Force measurements in E-cadherin-mediated cell doublets reveal rapid adhesion strengthened by actin cytoskeleton remodeling through Rac and Cdc42. *J Cell Biol* 167: 1183–1194, 2004. doi:10.1083/jcb.200403043.
10. **Churg A, Cosio M, Wright JL.** Mechanisms of cigarette smoke-induced COPD: insights from animal models. *Am J Physiol Lung Cell Mol Physiol* 294: L612–L631, 2008. doi:10.1152/ajplung.00390.2007.
11. **Couper D, LaVange LM, Han M, Barr RG, Bleecker E, Hoffman EA, Kanner R, Kleerup E, Martinez FJ, Woodruff PG, Rennard S; SPIROMICS Research Group.** Design of the Subpopulations and Intermediate Outcomes in COPD Study (SPIROMICS). *Thorax* 69: 491–494, 2014. doi:10.1136/thoraxjnl-2013-203897.
12. **David R, Luu O, Damm EW, Wen JW, Nagel M, Winklbauer R.** Tissue cohesion and the mechanics of cell rearrangement. *Development* 141: 3672–3682, 2014. doi:10.1242/dev.104315.
13. **de Jong PM, van Sterkenburg MA, Hesseling SC, Kempenaar JA, Mulder AA, Mommaas AM, Dijkman JH, Ponec M.** Ciliogenesis in human bronchial epithelial cells cultured at the air-liquid interface. *Am J Respir Cell Mol Biol* 10: 271–277, 1994. doi:10.1165/ajrcmb.10.3.8117445.
14. **Delgado O, Kaisani AA, Spinola M, Xie XJ, Batten KG, Minna JD, Wright WE, Shay JW.** Multipotent capacity of immortalized human bronchial epithelial cells. *PLoS One* 6: e22023, 2011. doi:10.1371/journal.pone.0022023.
15. **Herard AL, Zahm JM, Pierrot D, Hinnrasky J, Fuchey C, Puchelle E.** Epithelial barrier integrity during in vitro wound repair of the airway epithelium. *Am J Respir Cell Mol Biol* 15: 624–632, 1996. doi:10.1165/ajrcmb.15.5.8918369.
16. **Hogg JC, Timens W.** The pathology of chronic obstructive pulmonary disease. *Annu Rev Pathol* 4: 435–459, 2009. doi:10.1146/annurev.pathol.4.110807.092145.
17. **Inge LJ, Barwe SP, D'Ambrosio J, Gopal J, Lu K, Ryazantsev S, Rajasekaran SA, Rajasekaran AK.** Soluble E-cadherin promotes cell survival by activating epidermal growth factor receptor. *Exp Cell Res* 317: 838–848, 2011. doi:10.1016/j.yexcr.2010.12.025.
18. **Kasahara Y, Tuder RM, Taraseviciene-Stewart L, Le Cras TD, Abman S, Hirth PK, Waltenberger J, Voelkel NF.** Inhibition of VEGF receptors causes lung cell apoptosis and emphysema. *J Clin Invest* 106: 1311–1319, 2000. doi:10.1172/JCI10259.
19. **Kee YS, Robinson DN.** Micropipette aspiration for studying cellular mechanosensory responses and mechanics. *Methods Mol Biol* 983: 367–382, 2013. doi:10.1007/978-1-62703-302-2_20.
20. **Luo T, Mohan K, Iglesias PA, Robinson DN.** Molecular mechanisms of cellular mechanosensing. *Nat Mater* 12: 1064–1071, 2013. doi:10.1038/nmat3772.
21. **Maître JL, Berthoumieux H, Krens SF, Salbreux G, Jülicher F, Paluch E, Heisenberg CP.** Adhesion functions in cell sorting by mechanically coupling the cortices of adhering cells. *Science* 338: 253–256, 2012. doi:10.1126/science.1225399.
22. **Mathis C, Poussin C, Weisensee D, Gebel S, Hengstermann A, Sewer A, Belcastro V, Xiang Y, Ansari S, Wagner S, Hoeng J, Peitsch MC.** Human bronchial epithelial cells exposed in vitro to cigarette smoke at the air-liquid interface resemble bronchial epithelium from human smokers. *Am J Physiol Lung Cell Mol Physiol* 304: L489–L503, 2013. doi:10.1152/ajplung.00181.2012.
23. **Mège RM, Gavard J, Lambert M.** Regulation of cell-cell junctions by the cytoskeleton. *Curr Opin Cell Biol* 18: 541–548, 2006. doi:10.1016/j.ceb.2006.08.004.
24. **Milara J, Peiró T, Serrano A, Cortijo J.** Epithelial to mesenchymal transition is increased in patients with COPD and induced by cigarette smoke. *Thorax* 68: 410–420, 2013. doi:10.1136/thoraxjnl-2012-201761.
25. **Moussalli MJ, Wu Y, Zuo X, Yang XL, Wistuba II, Raso MG, Morris JS, Bowser JL, Minna JD, Lotan R, Shureiqi I.** Mechanistic contribution of ubiquitous 15-lipoxygenase-1 expression loss in cancer cells to terminal cell differentiation evasion. *Cancer Prev Res (Phila)* 4: 1961–1972, 2011. doi:10.1158/1940-6207.CAPR-10-0280.
26. **Murphy SL, Kochanek KD, Xu J, Heron M.** Deaths: Final Data for 2012. *Natl Vital Stat Rep* 63: 1–117, 2015.
27. **Oldenburger A, Poppinga WJ, Kos F, de Bruin HG, Rijks WF, Heijink IH, Timens W, Meurs H, Maarsingh H, Schmidt M.** A-kinase anchoring proteins contribute to loss of E-cadherin and bronchial epithelial barrier by cigarette smoke. *Am J Physiol Cell Physiol* 306: C585–C597, 2014. doi:10.1152/ajpcell.00183.2013.

28. **Olivera D, Knall C, Boggs S, Seagrave J.** Cytoskeletal modulation and tyrosine phosphorylation of tight junction proteins are associated with mainstream cigarette smoke-induced permeability of airway epithelium. *Exp Toxicol Pathol* 62: 133–143, 2010. doi:10.1016/j.etp.2009.03.002.
29. **Park GY, Christman JW.** Is the cellular response to cigarette smoke predictive of the phenotypic variation of COPD? *Am J Physiol Lung Cell Mol Physiol* 300: L809–L810, 2011. doi:10.1152/ajplung.00108.2011.
30. **Perrais M, Chen X, Perez-Moreno M, Gumbiner BM.** E-cadherin homophilic ligation inhibits cell growth and epidermal growth factor receptor signaling independently of other cell interactions. *Mol Biol Cell* 18: 2013–2025, 2007. doi:10.1091/mbc.E06-04-0348.
31. **Puchelle E, Zahm JM, Tournier JM, Coraux C.** Airway epithelial repair, regeneration, and remodeling after injury in chronic obstructive pulmonary disease. *Proc Am Thorac Soc* 3: 726–733, 2006. doi:10.1513/pats.200605-126SF.
32. **Rivera RM, Cosio MG, Ghezzo H, Salazar M, Pérez-Padilla R.** Comparison of lung morphology in COPD secondary to cigarette and biomass smoke. *Int J Tuberc Lung Dis* 12: 972–977, 2008.
33. **Schmid A, Baumlin N, Ivonnet P, Dennis JS, Campos M, Krick S, Salathe M.** Roflumilast partially reverses smoke-induced mucociliary dysfunction. *Respir Res* 16: 135, 2015. doi:10.1186/s12931-015-0294-3.
34. **Shaykhiev R, Otaki F, Bonsu P, Dang DT, Teater M, Strulovici-Barel Y, Salit J, Harvey BG, Crystal RG.** Cigarette smoking reprograms apical junctional complex molecular architecture in the human airway epithelium in vivo. *Cell Mol Life Sci* 68: 877–892, 2011. doi:10.1007/s00018-010-0500-x.
35. **Sidhaye VK, Chau E, Breysse PN, King LS.** Septin-2 mediates airway epithelial barrier function in physiologic and pathologic conditions. *Am J Respir Cell Mol Biol* 45: 120–126, 2011. doi:10.1165/rcmb.2010-0235OC.
36. **Stirbat TV, Mgharbel A, Bodennec S, Ferri K, Mertani HC, Rieu JP, Delanoë-Ayari H.** Fine tuning of tissues' viscosity and surface tension through contractility suggests a new role for α-catenin. *PLoS One* 8: e52554, 2013. doi:10.1371/journal.pone.0052554.
37. **Surcel A, Ng WP, West-Foyle H, Zhu Q, Ren Y, Avery LB, Krenc AK, Meyers DJ, Rock RS, Anders RA, Freel Meyers CL, Robinson DN.** Pharmacological activation of myosin II paralogs to correct cell mechanics defects. *Proc Natl Acad Sci USA* 112: 1428–1433, 2015. doi:10.1073/pnas.1412592112.
38. **Thorley AJ, Tetley TD.** Pulmonary epithelium, cigarette smoke, and chronic obstructive pulmonary disease. *Int J Chron Obstruct Pulmon Dis* 2: 409–428, 2007.
39. **Tuder RM, Petrache I, Elias JA, Voelkel NF, Henson PM.** Apoptosis and emphysema: the missing link. *Am J Respir Cell Mol Biol* 28: 551–554, 2003. doi:10.1165/rcmb.F269.
40. **Wang R, Ahmed J, Wang G, Hassan I, Strulovici-Barel Y, Hackett NR, Crystal RG.** Down-regulation of the canonical Wnt β-catenin pathway in the airway epithelium of healthy smokers and smokers with COPD. *PLoS One* 6: e14793, 2011. doi:10.1371/journal.pone.0014793.
41. **Winklbauer R.** Cell adhesion strength from cortical tension - an integration of concepts. *J Cell Sci* 128: 3687–3693, 2015. doi:10.1242/jcs.174623.
42. **Wong AP, Bear CE, Chin S, Pasceri P, Thompson TO, Huan LJ, Ratjen F, Ellis J, Rossant J.** Directed differentiation of human pluripotent stem cells into mature airway epithelia expressing functional CFTR protein. *Nat Biotechnol* 30: 876–882, 2012. doi:10.1038/nbt.2328.
43. **Woodruff PG, Barr RG, Bleecker E, Christenson SA, Couper D, Curtis JL, Gouskova NA, Hansel NN, Hoffman EA, Kanner RE, Kleerup E, Lazarus SC, Martinez FJ, Paine R III, Rennard S, Tashkin DP, Han MK; SPIROMICS Research Group.** Clinical Significance of Symptoms in Smokers with Preserved Pulmonary Function. *N Engl J Med* 374: 1811–1821, 2016. doi:10.1056/NEJMoa1505971.
44. **Wright JL, Cosio M, Churg A.** Animal models of chronic obstructive pulmonary disease. *Am J Physiol Lung Cell Mol Physiol* 295: L1–L15, 2008. doi:10.1152/ajplung.90200.2008.
45. **Wu SK, Gomez GA, Michael M, Verma S, Cox HL, Lefevre JG, Parton RG, Hamilton NA, Neufeld Z, Yap AS.** Cortical F-actin stabilization generates apical-lateral patterns of junctional contractility that integrate cells into epithelia. *Nat Cell Biol* 16: 167–178, 2014. doi:10.1038/ncb2900.
46. **Yap AS, Kovacs EM.** Direct cadherin-activated cell signaling: a view from the plasma membrane. *J Cell Biol* 160: 11–16, 2003. doi:10.1083/jcb.200208156.